Electron-beam lithography of plasmonic nanorod arrays for multilayered optical storage

Adam B. Taylor,[1] Pierrette Michaux,[1] Abu S. M. Mohsin,[1] and James W. M. Chon[1*]

[1]*Centre for Micro-Photonics, Faculty of Science, Engineering and Technology, Swinburne University of Technology, P. O. Box 218 Hawthorn 3122 Victoria Australia*
[*]*jchon@swin.edu.au*

Abstract: In this paper we demonstrate multilayer fabrication of plasmonic gold nanorod arrays using electron-beam lithography (EBL), and show that this structure could be used for multilayered optical storage media capable of continuous-wave (cw) laser readout. The gold nanorods fabricated using the EBL method are aligned perfectly and homogeneous in size and shape, allowing the polarization response of surface plasmon resonance (SPR) to be observed through ensemble array. This property in turn permits polarization detuned SPR readout possible and other manipulations such as progressively twisted arrays through the multilayers to make cw readout possible through deeper layers without too much extinction loss. The layered gold nanorod arrays are separated by thick spacer layer to enable the optical resolving of individual layers. Using this method, we demonstrated four-fold reduction in extinction loss for cw readout in three-layer structure. The current technique of multilayer fabrication and readout can be useful in 3-dimensional fabrication of plasmonic circuits and structures.

OCIS codes: (210.4810) Optical storage-recording materials; (240.6680) Surface plasmons; (220.4000) Microstructure fabrication; (220.4241) Nanostructure fabrication;

References and links

1. P. Zijlstra, J. W. M. Chon, and M. Gu, "Five-dimensional optical recording mediated by surface plasmons in gold nanorods," Nature **459**, 410-413 (2009).
2. J. W. M. Chon, C. Bullen, P. Zijlstra, and M. Gu, "Spectral encoding on gold nanorods doped in a silica sol-gel matrix and its application to high-density optical data storage," Advanced Functional Materials **17**, 875-880 (2007).
3. P. Zijlstra, J. W. M. Chon, and M. Gu, "Effect of heat accumulation on the dynamic range of a gold nanorod doped polymer nanocomposite for optical laser writing and patterning," Optics Express **15**, 12151-12160 (2007).
4. A. B. Taylor, J. Kim, and J. W. M. Chon, "Detuned surface plasmon resonance scattering of gold nanorods for continuous wave multilayered optical recording and readout," Optics Express **20**, 5069-5081 (2012).
5. M. Mansuripur, A. R. Zakharian, A. Lesuffleur, S. H. Oh, R. J. Jones, N. C. Lindquist, H. Im, A. Kobyakov, and J. V. Moloney, "Plasmonic nano-structures for optical data storage," Optics Express **17**, 14001-14014 (2009).
6. H. Ditlbacher, B. Lamprecht, A. Leitner, and F. R. Aussenegg, "Spectrally coded optical data storage by metal nanoparticles," Optics letters **25**, 563-565 (2000).
7. K. Ueno, V. Mizeikis, S. Juodkazis, K. Sasaki, and H. Misawa, "Optical properties of nanoengineered gold blocks," Optics Letters **30**, 2158-2160 (2005).
8. J. Wang, Y. T. Chen, X. Chen, J. M. Hao, M. Yan, and M. Qiu, "Photothermal reshaping of gold nanoparticles in a plasmonic absorber," Optics Express **19**, 14726-14734 (2011).
9. I. Ichimura, K. Saito, T. Yamasaki, and K. Osato, "Proposal for a multilayer read-only-memory optical disk structure," Applied Optics **45**, 1794-1803 (2006).
10. A. Mitsumori, T. Higuchi, T. Yanagisawa, M. Ogasawara, S. Tanaka, and T. Iida, "Multilayer 500 Gbyte optical disk," Japanese Journal of Applied Physics **48** (2009).
11. D. Dregely, K. Lindfors, J. Dorfmüller, M. Hentschel, M. Becker, J. Wrachtrup, M. Lippitz, R. Vogelgesang, and H. Giessen, "Plasmonic antennas, positioning, and coupling of individual quantum systems," Physica Status Solidi (B) Basic Research **249**, 666-677 (2012).

12. C. Novo, D. Gomez, J. Perez-Juste, Z. Zhang, H. Petrova, M. Reismann, P. Mulvaney, and G. V. Hartland, "Contributions from radiation damping and surface scattering to the linewidth of the longitudinal plasmon band of gold nanorods: A single particle study," Physical Chemistry Chemical Physics **8**, 3540-3546 (2006).
13. R. Gans, "Über die Form ultramikroskopischer Goldteilchen," Ann. Phys. **37**, 881-900 (1912).
14. S. W. Prescott, and P. Mulvaney, "Gold nanorod extinction spectra," Journal of Applied Physics **99**, 123504 (2006).

1. Introduction

Recently, plasmonic nanorod based multi-dimensional storage was demonstrated with storage capacity of up to Tbits/cm^3 [1-5], which can be useful for future archival-level storage as a long life time and low maintenance media. However, many challenges remain for its practical application [4]. Wet chemical synthesis of nanorods generally produces a large distribution in nanorod size and aspect ratio, which causes low signal-to-noise ratio. Random orientation, positioning and plasmon coupling also cause huge background fluctuation, making the readout less ideal.

Electron beam lithography (EBL) can provide much functionality that cannot be realised with wet chemical synthesis method. Control of nanorod dimension and alignment is possible, removing large randomness associated with wet chemical preparations. By controlling the pitch and orientation between nanorods single nanorods can act as single bits and increase the data density . In the past, Ditlbacher et al [6] first showed demonstration of optical storage on EBL fabricated rods. Ueno et al demonstrated precision EBL fabrication of the array of gold nanorods with controlled aspect ratio from 1 to 9 [7]. Qiu et al [8] also fabricated dense array of gold nano-rectangles for metamaterials.

Conventional EBL fabrication has been limited to a single layer, while modern high-density optical data storage (ODS) media is often produced in a multi-layer configuration to increase the storage capacity [9, 10]. Fabrication has been recently extended into the multilayer regime for nano-antenna application, using spin coating to produce dielectric spacer layers in between the metal elements [11]. However, optically resolving individual layers for this design is impossible as the spacer layers are on the order of tens of nanometers to allow plasmonic elements to interact. For the ODS media, each layer must be optically addressable without cross-talk from the neighbouring layers. Therefore the spacing of the layers must be greater than the axial resolution of the focussing objective, requiring spacing beyond 5μm.

Here, we demonstrate the production of axially resolvable multilayer optical storage media based on EBL fabricated gold nanorod array with photopolymer as a thick spacer layer. In doing so we experimentally demonstrate the low loss continuous-wave readout of multilayered storage media using polarization-detuned SPR readout method [4], which was previously impossible with wet-chemically synthesised, random gold nanorods. We employed SU-8 epoxy resin photoresist (Micro-Chem) as the spacer layer instead of pressure sensitive adhesive, due to its easy thickness control (10-30 μm thickness control by spin coating), optical quality (matching refractive index 1.52, low absorption), and chemical stability during EBL process. We successfully produced a three-layer structure and manipulated alignment of nanorod array in each layer to allow polarization-manipulated detuned SPR readout.

The paper is outlined as follows. In section 2, the theoretical consideration on detuned SPR polarization readout and required structures are proposed. In section 3, the EBL fabrication and characterization process are detailed, followed by optical readout results presented. In section 4, conclusions are provided.

2. Detuned SPR polarization readout on EBL fabricated multilayer sample – theoretical consideration

Recently detuned SPR readout method was proposed as a potential continuous-wave readout method for multilayered optical data storage [4]. In this scheme, data from multilayers is readout at slightly detuned wavelengths from SPR peak of gold nanorods (NRs) to avoid heavy beam extinction through the layers. Individual layers were found to have particular optimal wavelengths that could avoid the heavy beam extinction.

For optical drives, it is much more practical to detune in polarization space rather than in wavelength space. In this section, we present in detail the detuning in polarization dimension for continuous-wave multilayered optical recording medium based on EBL fabricated gold nanorods. In particular, we explore the case of progressively twisting the NR alignment through the layers to further reduce the loss during deeper layer readout.

Assuming that the recording medium consists of perfectly aligned array of plasmonic nanorods that are of single size and aspect ratio, the governing equation for the ratio ξ of scattering signal power to the input laser power takes the following form [4],

$$\xi^{SPR}(\theta, n) = \frac{P_s}{P_i} = \frac{NA^2}{\pi(0.61\lambda)^2}\sigma_s^{SPR}(\theta)\left[\exp(-N\sigma_e^{SPR}(\theta) - \alpha)\right]^{2(n-1)} \quad (1)$$

where σ_s^{SPR} and σ_e^{SPR} are scattering and extinction cross sections of gold nanorods at their SPR peak, N is the areal number density of the nanorods in single layer (NR number / unit area), and α is the residual absorbance of the spacer layer. The term inside the square bracket represents the transmittance through each layer, the 2(n-1) power index represents a number of layers that the readout beam traverses. The superscript *SPR* represents that the readout wavelength is at the SPR peak.

An exemplifying plot is shown in Fig. 1, where Fig. 1(a) shows a schematic of EBL fabricated multilayer structure, and Fig. 1(b) shows a plot of Eq.1, for a 10 layer structure with 15 x 45 nm spherically-capped cylinder nanorods and areal density of 2.5 x 10^9 cm^{-2} (centre to centre distance 200 nm, or 1 NR per 200 x 200 nm^2). The scattering and extinction cross sections are calculated using Mie-Gans analytical model with corrections [12-14].

Generally, σ_s and σ_e for NRs show $\cos^2\theta$ response with respect to irradiated light polarization. If the NRs are all aligned vertically throughout the layers (Fig.1(a)), the first layer readout will show the $\cos^2\theta$ response as expected. However, for subsequent layers the optimal peaks are shown to be detuned away from the vertical direction (0°, Fig. 1(b)), indicating it is more efficient to readout at detuned polarization angle as the layer number increases. The detuning angle reaches ~ 70° for the 10^{th} layer in this calculation, and at this angle the signal strength reaches 4 times more than that at no detuning angle (0°).

If the NRs are now twisted slightly at an angle ϕ from the preceding layer as shown in Fig. 1c, the Eq. 1 takes the following form,

$$\xi_{twisted}^{SPR}(\theta, n) = \frac{P_s}{P_i} = \frac{NA^2}{\pi(0.61\lambda)^2}\sigma_s^{SPR}(\theta)\prod_{i=1}^{n}\left[\exp(-N\sigma_e^{SPR}\cos^2(\theta - i\phi) - \alpha)\right]^2 \quad (2)$$

where the term $\cos^2(\theta - i\phi)$ accounts for the sequential twisting of NR alignment for each layer i, up to n. Fig. 1(d) shows the plot of Eq. 2 for 10 layer sample, with $\phi = 10^\circ$, (all the

other simulation parameters are identical to those for Fig. 1(b)) showing strong improvement in the signal strength at all the layers. In particular, result for layer 10 shows almost one order of magnitude higher scattering signal strength than without twisting (Fig. 1(b)), and from layers 5-9, the peak signal strengths are constant, something that is unachievable with conventional multilayered sample. In this rotated configuration, the optimum detuning angle is seen to still occur at angles detuned away from the nanorod orientation angle for each layer, though the required detuning is not as significant as that required for the aligned case.

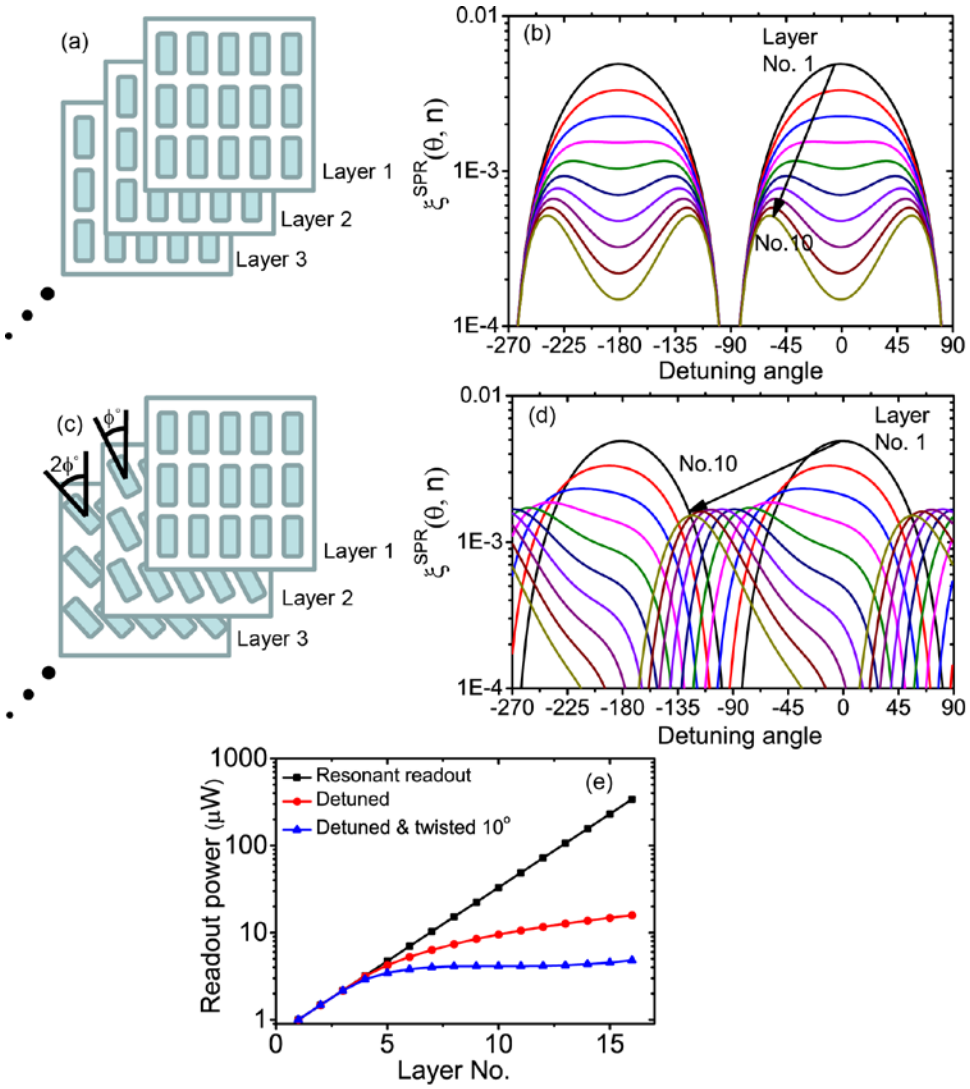

Fig. 1. The concept of detuned polarization continuous-wave readout on plasmonic nanorod based multilayered recording medium. (a) NRs are of single size and aligned in the same direction throughout the layers. (b) plot of scattering signal to input power ratio at SPR condition (ξ^{SPR}) from 1st layer to 10th layer for the NR sample shown in (a). In the first layer readout, the expected $\cos^2\theta$ response of NR scattering can be seen. However, for subsequent layer, optimum peak polarization for readout is shown to be detuned from 0 degree readout, due to heavy extinction at that angle. At 10th layer, the best readout is shown to be ~ 70 degrees. (c) NRs in this case are slightly twisted at an angle $\phi = 10^\circ$ progressively from first layer to the last layer. (d) plot of ξ^{SPR} from 1st layer to 10th layer for the twisted NR sample shown (c). NRs in this simulation are gold NRs, which have aspect ratio of 3 with width 15 nm, concentration of 2.5 x 10^9 NRs / cm^2. (e) Comparison of required readout power for equalized signal throughout the layers. Resonant SPR

readout, detuned, and detuned & twisted readout ($\phi = 10^{\circ}$) showing orders of magnitude improvement with detuned & twisted case.

Figure 1(e) shows the required laser input power to readout data with constant signal power. Exponential increase in input power is obvious for SPR readout at 0. For detuned readout, the power is reduced more than one order of magnitude at layer 16, and further reduction can be achieved for detuned and twisted case, only requiring 4-5 times the power required at the first layer to readout layer 16.

3. Multilayer gold nanorod array structure fabrication using electron-beam lithography

To demonstrate the detuned polarization SPR readout technique on multilayered array of gold nanorods, we firstly fabricated an array of gold nanorods with individual nanorods having dimensions of 30 x 90 nm, with 30 nm thickness, and 100 nm and 180 nm centre-to-centre spacing between rods in each direction using standard electron-beam lithography technique. In extending these arrays of aligned nanorods to a multilayer configuration, a spacer layer that satisfies multiple criterion is required: matching refractive index (n = 1.52) to the substrate and immersion medium, non-lossy, the ability to survive high temperature and vacuum during the EBL processing steps, ability to withstand the organic solvent lift-off process, relative stability during electron beam exposure, and the ease in quickly and cheaply producing ~ 20 μm thick coatings. The SU-8 photopolymer from Micro-Chem does satisfy all of the above criterion when spun-coat and cured.

A schematic of the multi-layer fabrication process is shown in Fig. 2. Once the nanorod array is fabricated, an SU-8 layer is deposited on top of the nanorod array and cured, which created a 20 μm thick spacer layer. This layer had necessary physical and chemical stability for the next EBL fabrication to proceed, and enabling subsequent layers to be fabricated above. This process was repeated to create 3 layer-structure.

Scanning electron microscopy (SEM, Fig. 2(a)) and optical imaging (Figs. 2(b) & 2(c)) was used to characterise the fabricated structures. The white-light scattering spectra from fabricated nanorods were measured, and compared with simulated spectrum using a commercial finite difference time-domain (FDTD) package, showing a good agreement, as seen in Fig. 2(a). The transmission optical image in Fig. 2(b) shows the three layers above one another, with layers below being slightly defocused.

Confocal laser scattering microscopy is used to characterise the scattering signal strength through the multilayer. The measurement was made using a home-built microscopy setup with a Ti:Sapphire laser (Tsunami, Spectra-Physics) as a tuneable laser source, from which continuous wave or pulsed operation could be chosen. The laser was spatially filtered using a pinhole, focused with a 1.4 NA objective (60 x Olympus) down onto the sample, which was mounted to a scanning stage (PI). Scattering based readout was collected by the same objective, and passed into a photo-multiplier tube (PMT, Oriel) with a pinhole. The position dependent scattering signal was then recorded by a home-built PC program.

The propagation of light through this multilayer is determined by shifting the focus of the objective through the sample in the z-direction. Figure 2(c) shows the scattering peaks from each nanorod layer. The strong decay observed in the peak intensity with the deeper layers is due to the large extinction caused by scattering and absorption of the light by the nanorods as it traverses the layers [4]. This extinction is experienced by the light in both directions of propagation, first as the laser is focussed down to the layer of interest, and again by the scattered light as it travels back up through the multilayer to the objective. Evidently, for many layered media, this extinction will be significant, needing large input powers to read data from the deeper layers [4]. The large contrast in the scattering intensity between the

peaks and the other areas indicates negligible cross-talk between the layers. The spacing between the layers would allow for a significantly lower NA objective to be used, such as used in optical drives, while still maintaining good inter-layer contrast.

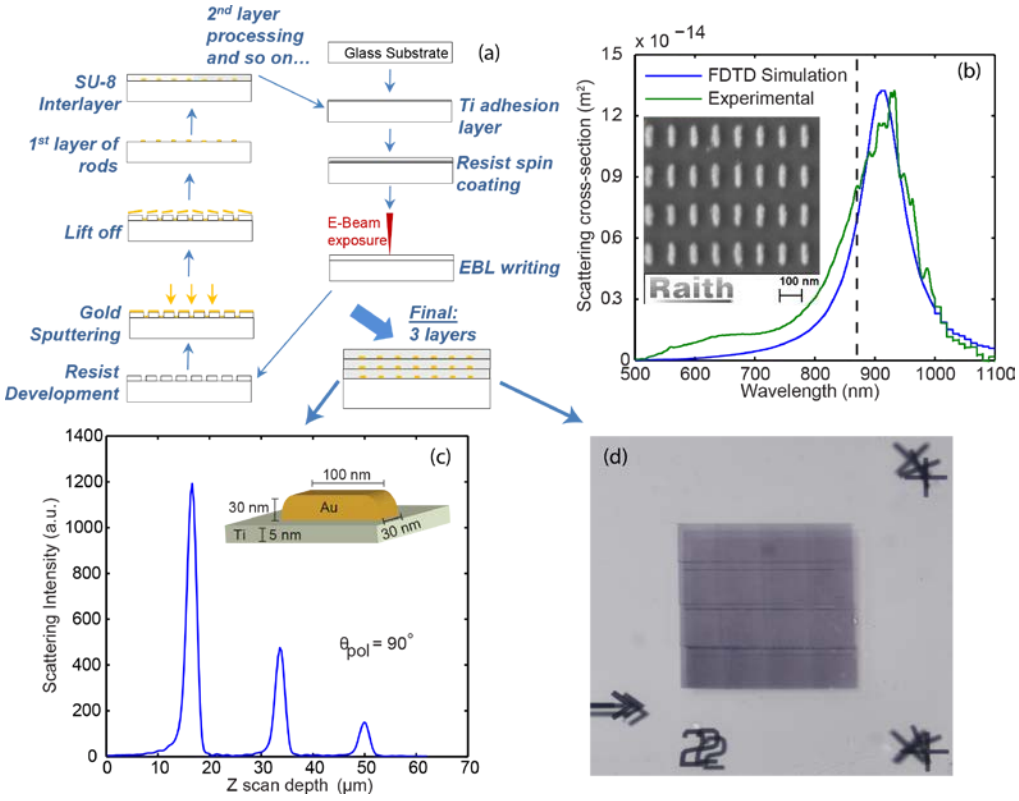

Fig. 2: (a) Schematic illustration of multilayer structure fabrication. Nanorods are fabricated onto a 5 nm Titanium adhesion layer, then overcoated with 20 μm of SU-8, with the process repeating for each layer. SEM image of fabricated nanorods, dimensions are measured as: 90nm long, 30nm wide, 30nm thick, with 180 nm center to center spacing. (b) Wide-field transmission optical image of a 3 layer nanorod array and alignment markers. All nanorods are aligned in the vertical direction in all layers. Defocus of lower layer alignment markers indicates the varying depth of the layers. A slight misalignment (~ 15 μm) was induced for better imaging. Side length of the array is 200 μm. (c) Collected depth dependent scattering measurements from multilayer, with 90° polarization, 1.4 NA oil immersion objective, and 870 nm wavelength.

In Section 2, Fig. 1(b), we have shown that strong decay in the collected signal at SPR can be mitigated by detuning the polarization angle (θ_{pol}) away from the orientation angle of the nanorods (δ_{NR}). This detuning can be further enhanced by rotating or "twisting" the orientation angle of the nanorods together with the laser polarization angle between each layer to further reduce the loss (see Fig. 1(c) & (d)). This idea is experimentally implemented using the current multilayer fabrication method.

Figure 3 shows scanning electron microscope (SEM) images of 3 layers fabricated in a multilayer configuration, using the techniques discussed above. The orientation angle of the nanorods in each layer is rotated progressively by 45°, resulting in the layers being oriented at

0°, 45°, and 90° for layers 1, 2 and 3 respectively. To image each layer, the polarization is adjusted to match the orientation angle of the nanorods in the layer of interest, resulting in the maximum scattering from the imaged layer, while minimizing the loss imparted by the upper layers.

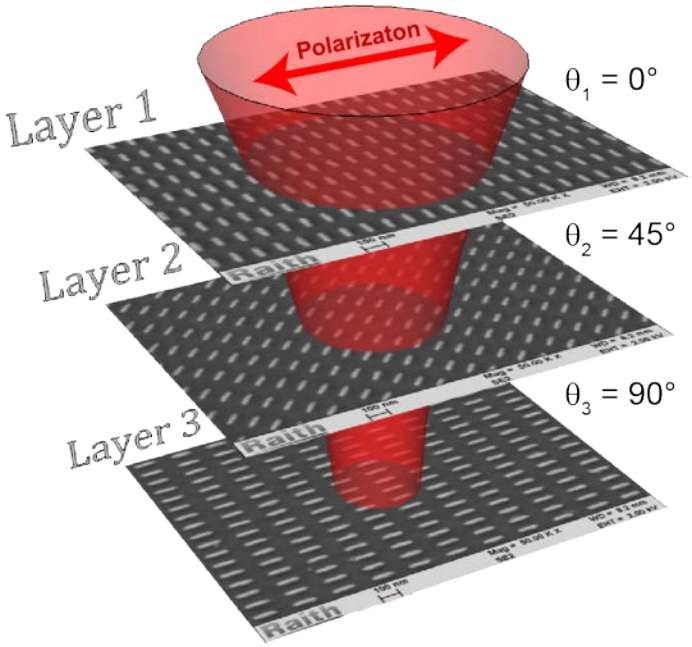

Fig. 3: SEM images of the nanorods fabricated within twisted multilayer geometry, with each array image taken before overcoating with SU-8. The nanorods in layers 1, 2, 3 are oriented at 0°, 45°, and 90° respectively. Overlaid cartoon illustrates how twisting mitigates the transit loss experienced by the polarized light, by reducing the apparent extinction coefficients of the nanorods in the upper layers, σext. The light is focused on layer 3, with the polarization direction represented by the red arrow, where the maximum scattering signal is generated.

To prove the effectiveness of this twisting technique, depth dependent scattering measurements are performed on each multilayer for a range of polarization angles between 0° and 180°. For each scan, the peak values are extracted and plotted as points. Fig. 4 shows results for the straight (a) and twisted (b) nanorod configurations. The depth scan is repeated at multiple x and y locations within the multilayer, to account for any spatial variation, with the mean signal being represented by the circles, and the error bars indicating the standard deviation of the results. This process can be theoretically modelled, with Eq. 1 representing the ratio of the final signal power to the input laser when the polarization is aligned to the nanorod long axis, θ_{NR}, an angle that is fixed for all layers. To model the twisted configuration and the effect of different laser polarizations, Equation 2 is used to account separately for the polarization component along θ_{NR}. Both polarization components experience reflection losses at the titanium interfaces which also must be included. The scattering and extinction cross sections of the nanorods at 870 nm were calculated from FDTD simulations, and have been used in Eq. 2 for modelling the present structures.

The theoretical results are overlaid onto the experimental data shown in Fig. 4, with the curves multiplied by a constant to match the intensity of the experimental points. Good agreement is observed between the theoretical and experimental results, indicating the theory correctly predicts the scattering signal strengths through the multilayered nanorod structure.

The readout power required for each layer in both straight alignment and twisted alignment case are measured, and the results are plotted below in Fig. 4(c), with the error bars indicating

the standard deviation of the measurements taken at multiple locations. The theoretically predicted values are also plotted, again showing good agreement to the experimental data. The strongly reduced loss imparted by the upper layers in twisted configuration is evident from Fig. 4(c), where a four-fold reduction in required power is seen at third layer, when compared to the straight configuration. The imaging powers for the deeper layers can be reduced by detuning the polarisation away from the orientation angle to the peak angle observed in Fig. 4(b) [4].

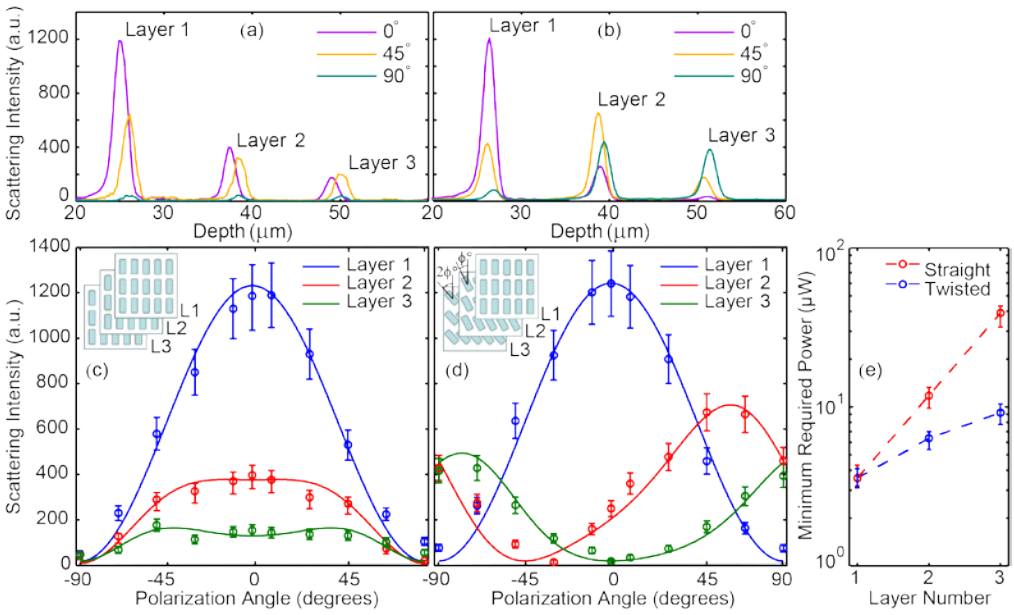

Fig. 4: (a) Experimental and theoretically obtained scattering intensities for a range of angles for readout from multilayer arrays of gold nanorods, where the nanorod orientation angle is kept constant between each layer. (b) Similar data for the twisted multilayer, where the angle of the nanorods changes between layers: 0°, 45° and 90° for layers 1, 2 and 3 respectively. (c) Experimental and theoretical readout powers required to achieve constant output on the detection PMT for various layers, with the polarization set to the match the orientation angle of the nanorods in each layer.

With the readout enhancement yielded by the twisted multilayer configuration established, optical patterning is then undertaken on each of the three layers to ensure data can be written and read on all after the multilayer fabrication process. For recording, a single shot, bit-by-bit recording was utilised at 6.4 mJ/cm^2 fluence, with the recording power being increased for deeper layers to account for single pass losses. Recording and readout was achieved using the same experimental configuration used for the previous scattering measurements. High focusing angle and large separation between the layers ensured that only nanorods within the focal volume experienced a fluence high enough for reshaping, without affecting nanorods in other layers. All recording was undertaken using a laser wavelength of 870 nm, with polarization aligned to the orientation angle of the nanorods in each layer. Readout on each layer was conducted using the same polarization angle and wavelength used for recording, and results are in Fig. 5. Evidently, successful recording is achievable on the nanorod arrays with excellent contrast, after subsequent fabrication of upper layers, proving the twisted configuration effectively supports the recording of data, while minimising the power required for reading this data out. Additionally, the recording of a separated series of bits was undertaken, with the results shown in Fig. 5(b), demonstrating simple detection of the written bits, with a signal to noise ratio of 5.1 ± 0.5.

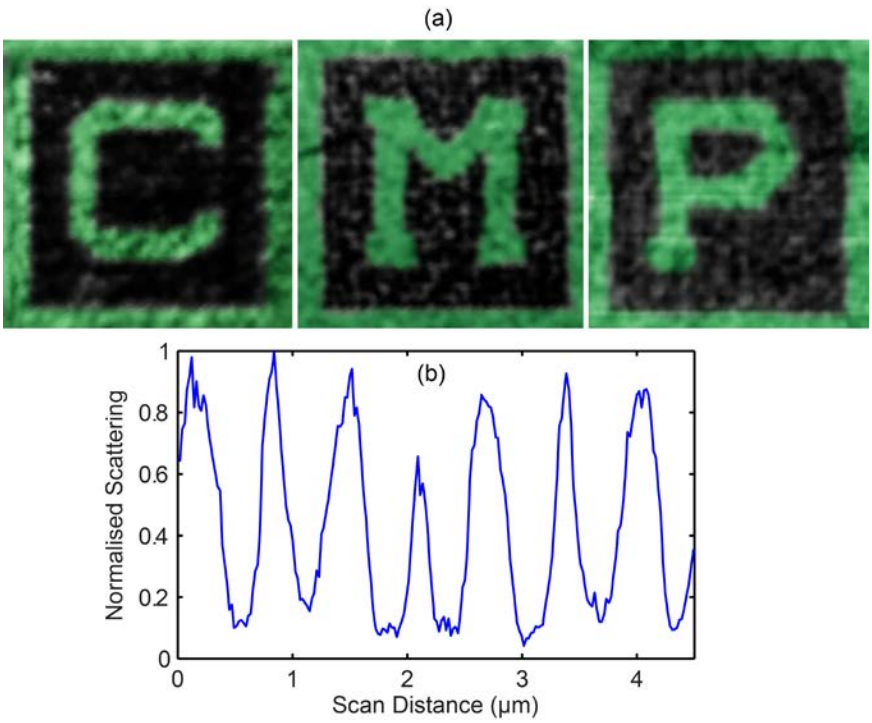

Fig. 5. (a) Confocal scattering images (15 μm x 15 μm image) obtained after single-pulse-per-pixel patterning of the nanorod arrays on the layers within the twisted configuration. Letter "C" was recorded on the layer 1, "M" on layer 2 and "P" on layer 3. Patterning was conducted using a wavelength of 870 nm, with the polarization adjusted to match θ_{NR} on each layer. (b) Bit trace cross-section along a series of fabricated bits, showing good recording contrast between written and un-written areas, and a high signal to noise ratio.

While we have used electron beam fabrication to form the twisted multilayer structures, nano-imprint lithography could also be used in place of EBL to form these structures. Nano-imprint lithography requires less production time and thus provides an effective solution for mass production of such nanorod based media. By forming a mold with the appropriate feature sizes, nanorod based media can be fabricated in a stamping process, whereby after a fabrication of single layer, the mold is rotated by some optimized angle, and the process is repeated. This process can be repeated as many times, with arrays being formed with each layer having a pre-defined orientation angle, such that the readout from the deeper layers is optimised.

4. Conclusions

In this paper we have demonstrated a novel technique whereby optically separate multilayers of nanorods can be fabricated by using a combination of SU-8 spin coating, and electron beam lithography. We have shown that by rotating the alignment angle of the nanorods between each layer, together with the polarization used for readout, the required readout powers can be minimised, by reducing the interlayer losses. Experimentally, this reduction was shown to be four-fold over 3 layers, and conceptually far higher for deeper layers, providing a technique to allow for deep layer readout with minimal laser power, while maintaining good recording contrast. Finally we have demonstrated that these multilayer nanorod arrays can be used for optical patterning, which can prove highly useful in areas such as high density archival data storage and cryptographic patterning on surfaces.

While we have used electron beam fabrication to form the twisted multilayer structures, nano-imprint lithography could also be used in place of EBL to form these structures. Nano-imprint lithography requires less production time and thus provides an effective solution for mass production of such nanorod based media. By forming a mold with the appropriate feature sizes, nanorod based media can be fabricated in a stamping process, whereby after a fabrication of single layer, the mold is rotated by some optimized angle, and the process is repeated. This process can be repeated as many times, with arrays being formed with each layer having a pre-defined orientation angle, such that the readout from the deeper layers is optimised. Finally, while we have demonstrated this proof of concept using 870 nm wavelength and gold nanorods, this operating wavelength can be reduced significantly by use of silver nanorods, in which the plasmon band can be tuned from 400 nm to 600 nm, in which the operating wavelength can be reduced to 405 nm, for integration into existing optical drives. The data density could then also reach beyond 1 Tbytes per CD/DVD sized disk with 1.2 mm thickness, assuming the spacer layer thickness is on the order of 10 μm.

Acknowledgment

We are grateful to Australian Research Council (DP 110102870, FT110101038) for the financial support for this project.